Published in final edited form as:
J Control Release. 2011 December 10; 156(2): 258–264. doi:10.1016/j.jconrel.2011.06.036.

In vivo distribution of surface-modified PLGA nanoparticles following intravaginal delivery

Yen Cu, PhD[1], **Carmen J. Booth, DVM, PhD**[2], and **W. Mark Saltzman, PhD**[1,§]
[1]Department of Biomedical Engineering, Yale University, USA
[2]Section of Comparative Medicine, School of Medicine, Yale University, USA

Abstract

Intravaginal (ivag) delivery, which is a proven way to confer local protection against STD's contracted via the reproductive tract, is complicated by the mucus gel barrier, the hormone cycle, and the harsh mucosal environment, which leads to low residence-time for administered agents. Polymer delivery vehicles may be useful in overcoming these barriers for delivery of agents. We explored the fate of nanoparticles (NP) made from poly(lactide-co-glycolide) (PLGA) in the mouse reproductive tract after ivag delivery. The nanoparticles were modified to display avidin (Avid-NP) or 2kDa PEG (PEG-NP) on their surface. Vaginal retention fractions for both muco-adhesive Avid-NP and stealthy PEG-NP were 5x higher than unmodified PLGA particles (NP). The amount of particles associated with mucus differed across formulations (Avid-NP>NP>PEG-NP). PEG-NP was found at higher concentration in the tissue than Avid-NP and NP up to 6 hr after delivery, and particles were found within epithelial cells and the underlying submucosal stromal and fibroblast cells of the vaginal tissue. Our results demonstrate that surface properties of nanoparticles can impact their fates following ivag delivery and that PEG-modified nanoparticles are potentially useful in ivag delivery.

Keywords

nanoparticle; mucosal; intravaginal delivery; fluorescence; surface modification

Introduction

The female reproductive tract is the initial site of viral pathogen exposure in many STDs. Therefore, some approaches to vaccination and antiviral therapy have delivered agents directly to this vulnerable mucosal surface. As examples, a recent study showed significant protection against HIV infection with a vaginal gel of the antiviral drug tenofovir [1] and mucosal immunization can induce humoral immunity both systemically and at the mucosal surface, which is an advantage over vaccines delivered by parenteral routes, which are usually capable of inducing only a systemic immune response [2, 3]. Formulation of agents for intravaginal (ivag) delivery must account for the anatomy and biological complexity of

[§]Corresponding author: W. Mark Saltzman, Department of Biomedical Engineering, MEC 414, Yale University, 55 Prospect St, New Haven, CT 06511, Phone: (203) 432 - 4262, Fax: (203) 432 - 0030, mark.saltzman@yale.edu.

The authors declare no conflict of interest

the tissue. Specifically, fluctuating hormone cycle and corresponding changes in tissue physiology [4], low residence time for soluble doses [5–7], mucus gel barrier, an acidic (pH ~3.8–4.2) environment which contains degradative enzymes [8, 9] leading to short half-life of biomolecules [10], and lack of inductive mucosal sites [11].

Viruses can infect the reproductive mucosa because they efficiently overcome these barriers to entry. Thus, one strategy for an ivag formulation is to mimic the design of a viral particle, which has been optimized through evolution. In one approach, agents are incorporated into virus-sized nanoparticles ($d < 200$ nm) composed of degradable polymers to protect the payload from the harsh environment and allow for their sustained release within target cells in the epithelium. The techniques for efficient encapsulation and engineering of release properties for polymer nanoparticles such as poly(lactide-co-glycolide) PLGA have been well-studied [12].

Polymer particles provide protection for their payload, and can be engineered to enhance their transport through the mucus barrier [13]. Furthermore, the size and surface properties of particles can be controlled, to influence their interaction with mucosal surface and penetration into the epithelium [14–20]. The enhanced efficacy (i.e., ability to induce immune response) of encapsulated vaccine formulations over soluble doses has been demonstrated *in vitro* with ovalbumin (OVA) [21], and *in vivo* with rE2 glycoprotein antigen [22] and plasmid DNA [23].

The surface properties of particles play a large role in their retention and transport in mucus [11]. While the use of mucoadhesive particles that bind to the mucus gel have been explored as a means to enhance particle retention in the lumen, it is not clear that these particles can efficiently reach therapeutic targets located beyond the mucus gel, such as within the epithelium or deeper (e.g., Langerhans cells and/or sub-mucosal dendritic cells) [24]. Alternately, it is known that some virus particles and other particles of net-neutral surface charge can effectively penetrate the mucus gel [25–27]. For example, small particles that are charge-neutral due to addition of a dense PEG coating were found to penetrate the epithelium after intranasal delivery at a higher rate than charged and/or larger sized particles [16]. This enhanced transport likely imparts higher efficacy for formulations carrying payload, as reported in recent studies using particles containing Hepatitis B antigen for intranasal [28] or OVA for oral [29] immunizations, where charge-neutral particles induced better immune responses over treatments with charged particles or soluble doses.

In addition, adhesion to mucus likely causes particles to be sloughed from the mucosal surface as mucus is shed. In a step towards the rational design of nanoparticles for intravaginal delivery, we identified two main obstacles to the transport of nanoparticles into reproductive tissue: a) retention within the lumen of the reproductive tract, and b) penetration of particles into the epithelium (Figure 1). Drugs administered in liquid (low-viscosity) formulations, such as is likely the case of nanoparticles, typically have low retention times due to gravitational forces and lack of anatomical structures to form an enclosed space, which permits leakage to the external environment. To reach the epithelial tissue, drugs must be retained in the reproductive tract for sufficient time to penetrate the mucus gel, which is a diffusional barrier that also reduces efficiency of drug delivery to the reproductive tract [30]. The barrier function of the mucus gel is two-fold: it serves as a sieve that filters out large molecules ($d > 1$ μm) and as a trap for molecules containing a surface charge. To arrive at the epithelium, particles must negotiate through the mucus gel, without becoming entangled in it, to reach the epithelium or else they are cleared from the lumen due to mucus turnover (1 ml/day at diestrus) [30]. We hypothesize that particle formulations that can best perform this function though mucus need to be small in size and possess specific surface properties that promote penetration into the tissue.

To test this hypothesis, we used both negatively-charged PLGA nanoparticles (NP) and mucoadhesive avidin-modified nanoparticles (Avid-NP): in an earlier study, we showed that these particles diffuse slowly through human cervical mucus [13]. We also showed that systematic modification of nanoparticles with PEG (PEG-NP) can improve their diffusion in cervical mucus. We examined the distribution of fluorescent nanoparticles with these different surface properties in the reproductive tract after ivag delivery. Lumen retention, interactions with mucus, and penetration of the particles into the tissue were also evaluated. The presence of nanoparticles within the lower reproductive tract and their association with different cell types was confirmed using fluorescent and brightfield imaging techniques.

Materials and Methods

Particle preparation

PLGA nanoparticles with distinct surface modifications were prepared and characterized as previously described [13]. Briefly, coumarin-6 (C6) was incorporated into the polymer using an emulsion/solvent removal method, with the C6 dissolved in organic phase at 3–4 % w/w. Formulated particles were stored at −20 °C until use.

Determination of coumarin-6 loading

Particles were dissolved at 5 mg/ml in DMSO. Fluorescence was measured in a quartz cuvette at 460/540nm, and the loading determined using a standard of known C6 concentration dissolved in DMSO and PLGA. For C6 release measurements, 3–5 mg nanoparticles was suspended in 1x PBS and incubated at 37 °C for 24 hrs. Particles were pelleted and dissolved in DMSO for determination of C6 retention.

Animal preparation

All procedures were approved by the Yale University Institutional Animal Care and Use Committee. Female C75Bl6 mice between 5–6 weeks were obtained from the National Cancer Institute. Mice were treated with Depo-Provera (Pharmacia & Upjohn Co.) by subcutaneous injection (2 mg/animal) 5 days prior to particle delivery. One day prior to delivery, the reproductive tract was extensively washed, by vaginal lavage with 1x PBS, to synchronize the content of mucus within the lumen.

Intravaginal delivery

Mice were anaesthetized under isoflurane (Baxter) using a vaporizer and nose cone apparatus. Fluorescent particles suspended at 50 mg/ml in 1x PBS were administered vaginally to each mouse at 15 μl/animal (750 μg nanoparticles). Mice were maintained under anesthesia in dorsal recumbency for 10 min after intravaginal instillation of particles.

Measurement of particle retention and lavage

To measure particle retention in the period after administration, mice were kept in a glass beaker lined with black absorbent paper. Each mouse was fitted with an Elizabethan collar (Promed-Tec Inc) to prevent self-grooming. After 0.5 hr, the paper lining was replaced. The second batch of paper was taken out at 2 hrs after initial delivery. The quality of particles deposited onto the absorbent paper cutouts were imaged using the IVIS 200 system (Xenogen). First, a threshold was set by the Living Image 3.0 software, and a region of interest (ROI) that encompassed the fluorescent area was determined and total fluorescent count measured. The fluorescent count per paper cutout was converted to mass of particles (μg nanoparticles) using a standard made from known amounts of particles. Fluorescent particle deposition on the face, fur and feet of mice were observed by eye.

Vaginal lavages were collected from mice at 0.5, 2, 6, and 24 hrs after administration by extensive vaginal lavage (4 washes each containing 50 μl of 1x PBS). In preliminary studies, we found that no additional fluorescent was recovered in lavages beyond the fourth; this is consistent with previous results, in which we showed that four washes were sufficient to remove ~100% of vaginally-administered IgG [10]. Fluorescence in lavage solutions was measured in a 96-well black plate (150 μl/well) using a multiplate reader at 460/540 nm. Fluorescent signals were converted to particle concentration using a standard prepared from known quantities of particles.

Tissue extraction and quantitation of particles

At selected times after vaginal lavage (t = 0.5, 2, 6, and 24 hrs after particle delivery), mice were placed under deep anesthesia and euthanized by cervical dislocation. The reproductive tissues were harvested, weighed and homogenized on ice in DMSO at 10% w/v. Homogenate was vortexed for 4–5 hrs and the solid content pelleted by centrifugation. The fluorescence in the supernatant was read at 460/540 nm and converted particle concentration using a standard made of known amount of particles in DMSO.

Necropsy and Histopathology

Nanoparticles (NP, Avid-NP, PEG-NP) were administered vaginally as described above; in addition, control mice were untreated or treated with non-fluorescent nanoparticles (no C6). Mice were euthanized by CO_2 asphyxiation at 6 hrs after delivery. Tissues were harvested and fixed in Bouin's fixative (Ricca Chemical Corporation, Arlington TX), processed, embedded in paraffin, sectioned at 5 μm, and stained with toluidine blue (T Blue) by routine methods. T Blue-stained sections were examined at 60x magnification on a fluorescent microscope for the presence of nanoparticles on a AxioImager.A1 (Zeiss, Germany); cellular localization was determined by a reviewer blind to the experimental manipulation. T Blue digital light microscopic images of the same section were taken on a Zeiss Axioskop microscope, AxoCam MRc5 camera and AxioVision 4.7.1 imaging software (Carl Zeiss Micro Imaging, Inc. Thornwood, NY). Images were optimized in Adobe® Photoshop® (Adobe Systems Incorporated, San Jose, California).

Statistical analysis

Unpaired student t-tests were performed on samples using GraphPad Prism v5 software. Criteria for statistical significance was determined as noted for each respective data set.

Results

All nanoparticle preparations encapsulating C6 dye consisted of small, spherical particles. Despite differences in surface modification, there were no differences in surface morphology (Figure 2). The size distribution (d ~ 150–170 nm), surface zeta-potential, and aggregation tendencies of these particles have been reported previously [13]. When incubated in PBS, negligible quantities of C6 are released from the particles (samples contained 0.17±0.1 μg C6/mg PLGA prior to incubation and 0.18±0.2 μg C6/mg PLGA after 24 hr incubation). We characterized C6 particles extensively in earlier work, showing that they can be identified by multiphoton microscopy in tissues as individual particles with negligible release of C6 [31].

A total dose of 750 μg of particles was introduced into the lower reproductive tracts of C57Bl/6 female mice, which were previously induced to diestrus by Depo-Provera, a long-lasting progestin. The fate of particles after ivag delivery was measured by tracking of fluorescence signal and classified as shown in Fig. 1: collection on absorbent paper

(leakage), vaginal lavage (mucus-association), fluorescence extraction from tissue homogenate (tissue penetration) and imaging of reproductive tissue (cell association).

We hypothesize that the amount of fluorescence spotted onto black absorbent paper underneath freely mobile mice is indicative of the extent of particle leakage from the reproductive tract. A standard curve using known quantities of nanoparticles spotted onto the absorbent paper was used to convert the fluorescence signal on sample papers into mass (μg) of nanoparticles deposited (Figure 3A, B). For each mouse, two paper blots were collected, which represents two time intervals: 0–0.5 hr and 0.5–2 hr (Figure 3C). The majority of spotting occurred within the first 30 min; leakage was significantly higher for unmodified NP's (99 ± 18 μg) compared to Avid-NP at 22 ± 3.5 μg and PEG-NP at 25 ± 4.7 μg (Figure 3D). All sample distributions were skewed to the left, such that the medians of the measurements were lower, at 51, 11, and 9.7 μg for NP, Avid-NP and PEG-NP, respectively (Table 1). Between 0.5 and 2 hrs, much less leakage (0.2 – 0.5 μg of particles) was detected from mice receiving NP and Avid-NP, and none was detected from mice receiving PEG-NP.

Nanoparticles were collected by vaginal washes at various time points after delivery (Figure 4). The highest quantity of nanoparticles recovered by lavage after 0.5 hrs was for mice administered with Avid-NP (320 ± 46 μg nanoparticles/mouse); smaller quantities were found for mice receiving NP (220 ± 32 μg) or PEG-NP (170 ± 41 μg). The differences between animals treated with Avid-NP and NP ($p < 0.10$) or PEG-NP ($p < 0.025$) were statistically significant. The quantity of particles collected by vaginal washing was less at 2 hrs than 0.5 hrs. The quantities of particles recovered from both NP and Avid-NP treated animals (66 ± 15 and 60 ± 15 μg, respectively) were statistically higher than those treated with PEG-NP (23 ± 5.7 μg) at this time point. At 6 hrs after delivery, between 15 and 30 μg nanoparticles were found in the lumen of the reproductive tract; at 24 hr, between 1 and 4 μg were found; there were not significant differences between the groups at these times.

The reproductive tracts of mice were harvested after extensive vaginal washing. Fluorescence imaging of the excised reproductive organ revealed that the majority of particles were found in the vaginal lumen (Figure 5A). The fluorescent signal was highest within the lower reproductive tract and decreased with time after administration; after 24 hrs, no fluorescence signals were detected (Figure 5B). Fluorescent particles were extracted from tissue homogenates in DMSO (Figure 5C). At 0.5 hrs after administration, between 10–30 μg nanoparticles/mouse were measured; fewer particles were detected at each subsequent time point. PEG-NP was found at higher concentration within tissues, as compared to Avid NP and NP, across all time points. This difference between PEG-NP and other formulations was statistically significant at 6 hrs. At 24 hrs, no fluorescence was detected in any animals. We did not find fluorescence in the draining lymph nodes adjacent to the reproductive tract or in the peritoneal cavity.

The presence of nanoparticles within fixed tissue sections was observed by fluorescent and brightfield imaging for animals sacrificed 6 hrs after administration (Figure 6). No fluorescence was detected in sections from animals that were untreated or treated with blank (no C6) nanoparticles (Figure 6A, B). However, fluorescence particles (which appeared as bright dots, indicated with solid white arrows) were detected within sections of tissue from animals treated with fluorescent NP, Avid-NP and PEG-NP (Figure 6C, D, E). Using the corresponding brightfield images of the same section, we confirmed that the nanoparticles were associated with a variety of cell types within the vaginal tissue (i.e., epithelial cells, fibroblasts and submucosal stromal cells). Cells were identified by their location in the tissue and their morphological characteristics: while we are confident in these classifications —based on our extensive previous experience with cell identification in mouse reproductive

tissues, we also recognize that more definitive characterization can be done by co-localization with cell specific biochemical markers. All tissues examined, including tissues from animals treated with all three nanoparticle formulations, appeared normal and without inflammation.

Discussion

In premenopausal human adults, the thickness of the vaginal epithelium fluctuates during the menstrual cycle, changing as much as 200–300 μm [32]. The mouse reproductive mucosa is most permeable at diestrus due to the thinned cell lining after the shedding of the endometrium and the increased hydration of the mucus gel. Our study utilizes the mouse as an *in vivo* model to evaluate mucosal delivery in the reproductive tract. While the mouse diestrus state is not accompanied by the shedding of an endometrial layer as in humans, and humans do not experience diestrus, it has been shown that the mucosa of mice at diestrus is relevant for study of vaginal delivery of therapeutics [7, 33] and—although an imperfect replica—results from mice can be translated to humans. In this study, delivery of nanoparticles was performed on mice at diestrus, which was induced by subcutaneous injection of Depo-Provera, a long-lasting progestin.

Unmodified PLGA particles (NP) exhibited significantly lower retention in the lumen after ivag delivery than particles modified with avidin or PEG (Figure 3C). For NP formulation, ~13 % of the delivered dose was lost during the 30 min after delivery, which was 5x higher than either Avid-NP or PEG-NP. No spotting events were detected between 0.5–2 hrs (Figure 3D). Experiments to monitor leakage were not extended beyond 2 hrs due to discomfort of the animals, ingestion of the paper, and excretions that collected on the paper, decreasing the reliability of the measurements. The majority of fluorescent spots on the paper appeared as distinct (not smeared) areas, due to the quick absorption of liquid, and no appreciable deposition of particles on the fur or feet of mice was detected visually. As a control, similar known amounts of particles were deposited onto absorbent paper such that each sample occupied different surface areas. The same resulting total signal was calculated for all areas, which confirmed the accuracy of the fluorescence count algorithm used by the imaging software.

Particles collected by vaginal washes at each time point strongly associated with the mucus gel, such that the mucus recovered from the lumen—which appeared as distinct and viscous globules within the wash solution—were brightly colored with particles. Avid-NP, a mucoadhesive formulation, was found to have highest association with mucus gel at 0.5 hr, followed by NP and PEG-NP (Figure 4). We believe that the low concentration of NP measured at this time point was partly due to its high leakage after delivery. PEG-NP formulations, which were shown previously to diffuse most rapidly through mucus [13], exhibited significantly lower concentration in the washes at 0.5 and 2 hr, which we believe is due to its reduced association with mucus. Nanoparticle concentrations in the lumen decreased over time, and approached background level after 24 hrs.

PEG-NP particles were found at significantly higher concentration in the reproductive tissues, beyond the mucus layer, at 2 and 6 hr after intravaginal delivery (Figure 5). The particles were mainly localized in the lower reproductive tract, (Figure 5A, B). Due to the limit of detection using this imaging technique, no fluorescence signal was detected from the extracted reproductive organs after 24 hrs. Fluorescence recovered from tissue homogenates (Figure 5C) was on average higher for PEG-NP than Avid-NP and NP formulations. This difference in concentration was significant at 6 hrs, and no particles were detected from the tissue at 24 hrs. The total fluorescence signal recovered from tissue, though significantly above background, was overall low. Compared to a control sample where untreated tissues

were spiked with known amount of particles and extracted using the same method, the efficiency of fluorescence extraction was ~50%. This factor was used to correct the fluorescent signal measured from tissue homogenates.

Toluidine Blue (T Blue) was used for histopathology study (Figure 6), due to its low level of auto-fluorescence, which might interfere with the fluorescence images. While some tissue autofluorescence was present in our images, the nanoparticles appeared as bright dots that were readily distinguishable from the background. With the combination of both fluorescence and brightfield imaging techniques, we confirmed the co-localization of nanoparticles within different cell types of the reproductive tissue.

The total particle mass recovered on absorbent paper (which we attribute to leakage), by vaginal washing (which we attribute to association with mucus in the vaginal lumen), and within tissue homogenates (which we attribute to particles that have penetrated into the epithelial tissue) was 30–49% of the initially delivered nanoparticle dose at t = 0.5 hr, and 8–22 % at t = 2 hr (Table 2). No leakage was detected during the period from 0.5 to 2 hrs. Because no data on leakage is available after 2 hrs, it is less clear about the fate of particles beyond this time point. It is possible that particles associated with the mucus gel continue to be expelled from the tract between 2–24 hrs due to mucus turnover, although we predict that only small amounts would be cleared from the mouse by this route. In addition, fluorescence measurements from the digestive tract were not taken, and the fraction of particles unaccounted for may be a consequence of self-grooming by the mice, which were awake and active during the observation period. We were unable to account for all of the administered particles using these techniques, but that has been a common finding in studies of ivag administration. Sakaguchi *et al*. determined that the majority (~75 %) of ^{14}C labeled sodium plasterone sulphate administered ivag to rats was excreted in the urine and feces within the first 24 hrs [7]; in this situation, the drug was absorbed through the reproductive mucosa, circulated in the blood and was then eliminated by hepatic and renal mechanisms. Fowler *et al*. delivered ^{125}I and ^{14}C labeled nonoxynol-9 to anesthetized rats and measured the drug distribution over time. After 6 hrs, only 48 % of ^{125}I-labeled and 82 % of the total delivered dose of ^{14}C labeled drug could be accounted for. The highest concentration of nonoxynol-9 was found in the reproductive tract [6]. Chatterton *et al*. treated human subjects intravaginally with 99mTc-DTPA labeled cream and gel formulations and measured radioactivity recovered in sanitary napkins and *in vivo* by gamma scintigraphy. Of the total dose, only 54 % (cream) and 62 % (gel) could be accounted for after 24 hrs. In addition, the retention of soluble drugs was found to be highly variable between subjects (1–81 %) and strongly dependent on frequency of urination and bowel activities [5].

Conclusion

The surface of the female reproductive tract contains physical and chemical barriers that pose a challenge to agent action after ivag delivery. We show here that delivery to the female reproductive tract can be improved using rationally designed polymeric carriers made from FDA-approved materials, namely PLGA and PEG. The size and surface of these particles can be manipulated to overcome physical barriers such as the mucus gel. Our findings revealed that PEG-NP, which have a net-neutral surface but penetrate mucus most rapidly, and Avid-NP, which are mucoadhesive, do not undergo leakage after ivag delivery to the same extent as unmodified PLGA nanoparticles (NP, negatively-charged). Furthermore, PEG-NP can more efficiently penetrate the mucosal epithelium, such that it was found at higher concentration in the tissue over time. These PEG-NP vehicles might be significantly more effective for delivery of agents that require vehicles to facilitate entry into cells for biological effectiveness, such as siRNA, plasmid DNA, or some vaccinogens. Our

study presents a polymer nanoparticle formulation, rationally designed to have enhanced transport properties, that has potential applications in ivag drug delivery.

Acknowledgments

Supported by a grant from the National Institute of Health (EB000487). We thank Professor Richard Flavell and his laboratory for use of the IVIS instrument.

References

1. Karim QA, Karim SSA, Frohlich JA, Grobler AC, Baxter C, Mansoor LE, Kharsany ABM, Sibeko S, Mlisana KP, Omar Z, Gengiah TN, Maarschalk S, Arulappan N, Mlotshwa M, Morris L, Taylor D, Grp CT. Effectiveness and Safety of Tenofovir Gel, an Antiretroviral Microbicide, for the Prevention of HIV Infection in Women. Science. 2010; 329(5996):1168–1174. [PubMed: 20643915]
2. Walker RI. New strategies for using mucosal vaccination to achieve more effective immunization. Vaccine. 1994; 12(5):387–400. [PubMed: 8023545]
3. Kuo-Haller P, Cu Y, Blum J, Appleton JA, Saltzman WM. Vaccine Delivery by Polymeric Vehicles in the Mouse Reproductive Tract Induces Sustained Local and Systemic Immunity. Mol Pharm. 2010; 7(5):1585–1595.
4. Parr, MB.; Parr, EL. Handbook of Mucosal Immunology. Ogra, PL.; Mestecky, J.; Lamm, ME.; Strober, W.; McGee, JR.; Bienenstock, J., editors. Academic Press, Inc; San Diego: 1994. p. 677-689.
5. Chatterton BE, Penglis S, Kovacs JC, Presnell B, Hunt B. Retention and distribution of two 99mTc-DTPA labelled vaginal dosage forms. Int J Pharm. 2004; 271(1–2):137–143. [PubMed: 15129980]
6. Fowler PT, Matsumoto K, Page RC, Digenis GA. Synthesis of novel iodinated derivatives of nonoxynol-9 and their bioavailability in rats. Nucl Med Biol. 2002; 29(7):771–775. [PubMed: 12381457]
7. Sakaguchi M, Sakai T, Adachi Y, Kawashima T, Awata N. The biological fate of sodium prasterone sulfate after vaginal administration. I. Absorption and excretion in rats. J Pharmacobiodyn. 1992; 15(2):67–73. [PubMed: 1403604]
8. Woolfson AD, Malcolm RK, Gallagher R. Drug delivery by the intravaginal route. Crit Rev Ther Drug Carrier Syst. 2000; 17(5):509–555. [PubMed: 11108158]
9. Lee VH. Enzymatic barriers to peptide and protein absorption. Crit Rev Ther Drug Carrier Syst. 1988; 5(2):69–97. [PubMed: 3052875]
10. Sherwood JK, Zeitlin L, Chen X, Whaley KJ, Cone RA, Saltzman WM. Residence half-life of IgG administered topically to the mouse vagina. Biol Reprod. 1996; 54(1):264–269. [PubMed: 8838025]
11. Mestecky J, Moldoveanu Z, Russell MW. Immunologic uniqueness of the genital tract: challenge for vaccine development. Am J Reprod Immunol. 2005; 53(5):208–214. [PubMed: 15833098]
12. Mundargi RC, Babu VR, Rangaswamy V, Patel P, Aminabhavi TM. Nano/micro technologies for delivering macromolecular therapeutics using poly(D,L-lactide-co-glycolide) and its derivatives. J Control Release. 2008; 125(3):193–209. [PubMed: 18083265]
13. Cu Y, Saltzman WM. Controlled surface modification with poly(ethylene)glycol enhances diffusion of PLGA nanoparticles in human cervical mucus. Mol Pharm. 2009; 6(1):173–181. [PubMed: 19053536]
14. Behrens I, Pena AI, Alonso MJ, Kissel T. Comparative uptake studies of bioadhesive and non-bioadhesive nanoparticles in human intestinal cell lines and rats: the effect of mucus on particle adsorption and transport. Pharm Res. 2002; 19(8):1185–1193. [PubMed: 12240945]
15. Tabata Y, Inoue Y, Ikada Y. Size effect on systemic and mucosal immune responses induced by oral administration of biodegradable microspheres. Vaccine. 1996; 14(17–18):1677–1685. [PubMed: 9032899]

16. Vila A, Gill H, McCallion O, Alonso MJ. Transport of PLA-PEG particles across the nasal mucosa: effect of particle size and PEG coating density. J Control Release. 2004; 98(2):231–244. [PubMed: 15262415]

17. Dhaliwal S, Jain S, Singh HP, Tiwary AK. Mucoadhesive microspheres for gastroretentive delivery of acyclovir: in vitro and in vivo evaluation. AAPS J. 2008; 10(2):322–330. [PubMed: 18523891]

18. Takeuchi H, Matsui Y, Sugihara H, Yamamoto H, Kawashima Y. Effectiveness of submicron-sized, chitosan-coated liposomes in oral administration of peptide drugs. Int J Pharm. 2005; 303(1–2):160–170. [PubMed: 16125348]

19. Yamamoto H, Kuno Y, Sugimoto S, Takeuchi H, Kawashima Y. Surface-modified PLGA nanosphere with chitosan improved pulmonary delivery of calcitonin by mucoadhesion and opening of the intercellular tight junctions. J Control Release. 2005; 102(2):373–381. [PubMed: 15653158]

20. Yin Y, Chen D, Qiao M, Wei X, Hu H. Lectin-conjugated PLGA nanoparticles loaded with thymopentin: ex vivo bioadhesion and in vivo biodistribution. J Control Release. 2007; 123(1):27–38. [PubMed: 17728000]

21. Shen H, Ackerman AL, Cody V, Giodini A, Hinson ER, Cresswell P, Edelson RL, Saltzman WM, Hanlon DJ. Enhanced and prolonged cross-presentation following endosomal escape of exogenous antigens encapsulated in biodegradable nanoparticles. Immunology. 2006; 117(1):78–88. [PubMed: 16423043]

22. Brandhonneur N, Loizel C, Chevanne F, Wakeley P, Jestin A, Le Potier MF, Le Corre P. Mucosal or systemic administration of rE2 glycoprotein antigen loaded PLGA microspheres. Int J Pharm. 2009; 373(1–2):16–23. [PubMed: 19429284]

23. Khatri K, Goyal AK, Gupta PN, Mishra N, Vyas SP. Plasmid DNA loaded chitosan nanoparticles for nasal mucosal immunization against hepatitis B. Int J Pharm. 2008; 354(1–2):235–241. [PubMed: 18182259]

24. Iwasaki A. Mucosal dendritic cells. Annu Rev Immunol. 2007; 25:381–418. [PubMed: 17378762]

25. Wang YY, Lai SK, Suk JS, Pace A, Cone R, Hanes J. Addressing the PEG Mucoadhesivity Paradox to Engineer Nanoparticles that “Slip” through the Human Mucus Barrier. Angew Chem Int Ed Engl. 2008

26. Lai SK, O’Hanlon DE, Harrold S, Man ST, Wang YY, Cone R, Hanes J. Rapid transport of large polymeric nanoparticles in fresh undiluted human mucus. Proc Natl Acad Sci U S A. 2007; 104(5):1482–1487. [PubMed: 17244708]

27. Olmsted SS, Padgett JL, Yudin AI, Whaley KJ, Moench TR, Cone RA. Diffusion of macromolecules and virus-like particles in human cervical mucus. Biophys J. 2001; 81(4):1930–1937. [PubMed: 11566767]

28. Thomas C, Gupta V, Ahsan F. Influence of surface charge of PLGA particles of recombinant hepatitis B surface antigen in enhancing systemic and mucosal immune responses. Int J Pharm. 2009

29. Slutter B, Plapied L, Fievez V, Sande MA, des Rieux A, Schneider YJ, Van Riet E, Jiskoot W, Preat V. Mechanistic study of the adjuvant effect of biodegradable nanoparticles in mucosal vaccination. J Control Release. 2009; 138(2):113–121. [PubMed: 19445980]

30. Cone RA. Barrier properties of mucus. Adv Drug Deliv Rev. 2009; 61(2):75–85. [PubMed: 19135107]

31. Woodrow KA, Cu Y, Booth CJ, Saucier-Sawyer J, Wood MJ, Saltzman WM. Intravaginal gene silencing using biodegradable nanoparticles densely loaded with small-interfering RNA. Nature Materials. 2009; 8:526–533.

32. Hussain A, Ahsan F. The vagina as a route for systemic drug delivery. J Control Release. 2005; 103(2):301–313. [PubMed: 15763615]

33. Kanazawa T, Takashima Y, Hirayama S, Okada H. Effects of menstrual cycle on gene transfection through mouse vagina for DNA vaccine. Int J Pharm. 2008; 360(1–2):164–170. [PubMed: 18573624]

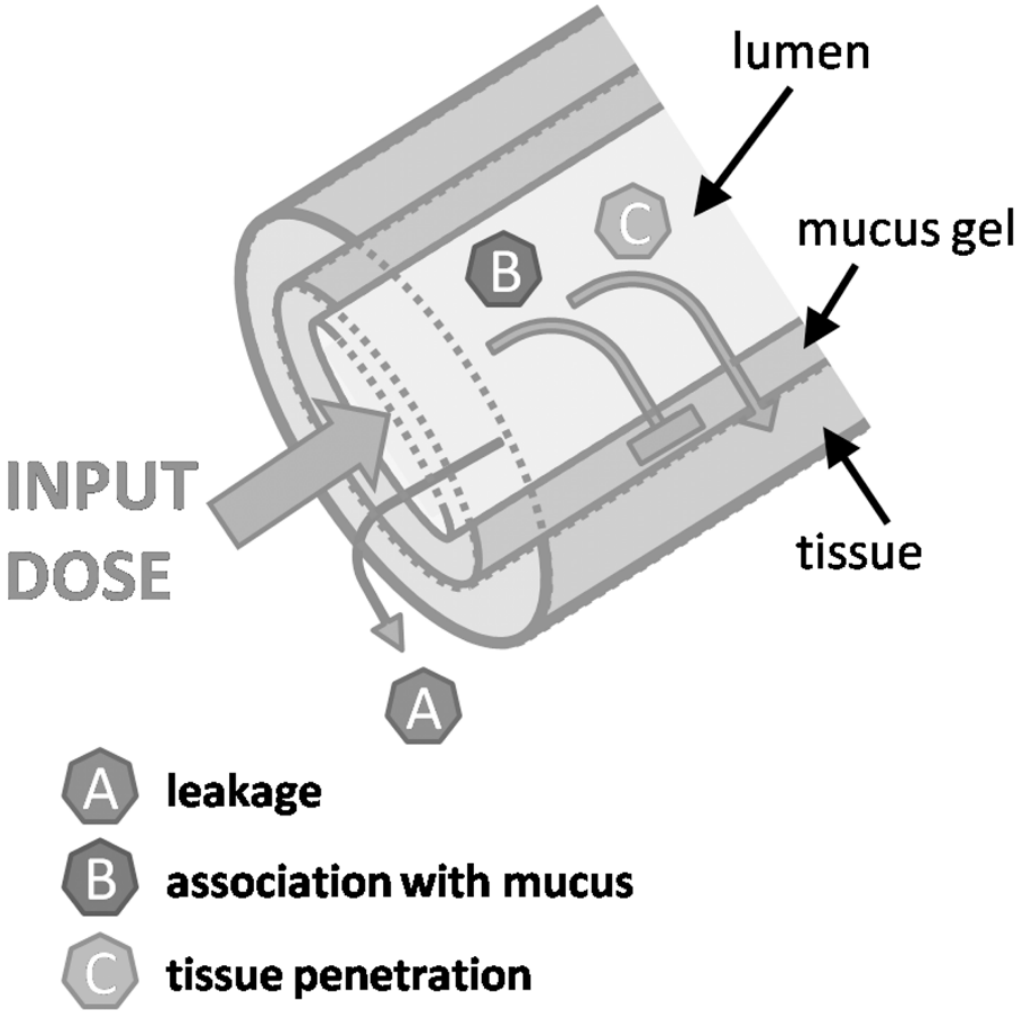

Figure 1.
The distribution of a formulation delivered by ivag administration is classified into 3 main fates. After administration into the lumen, the agent can: A) leak from the body; B) associate with the mucus gel on top of the epithelium, which hinders further penetration into the body; or C) penetrate the mucus gel to reach the underlying cells.

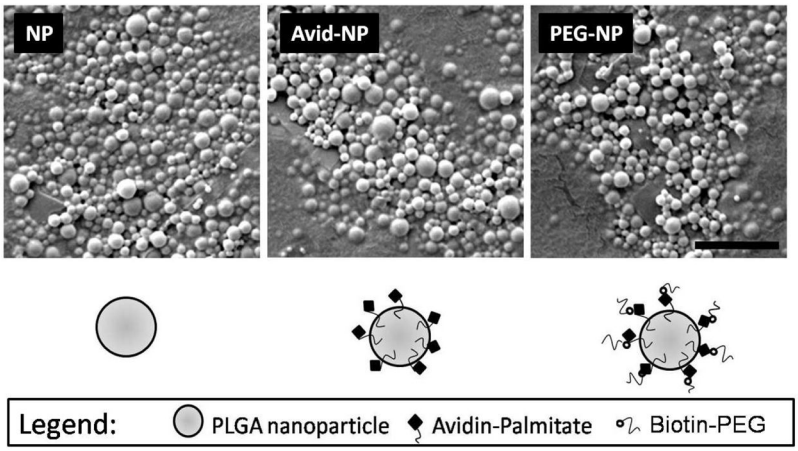

Figure 2.

Particle morphology and schematic of surface modifications. PLGA nanoparticles (d~150–170nm) with no surface modifications (NP), surface modification with avidin-palmitate conjugate (Avid-NP) and surface modification with biotin-2kDa PEG (PEG-NP) were made with 1.7 ± 0.14 % w/w coumarin-6 loading. Scale bar: 1 μm

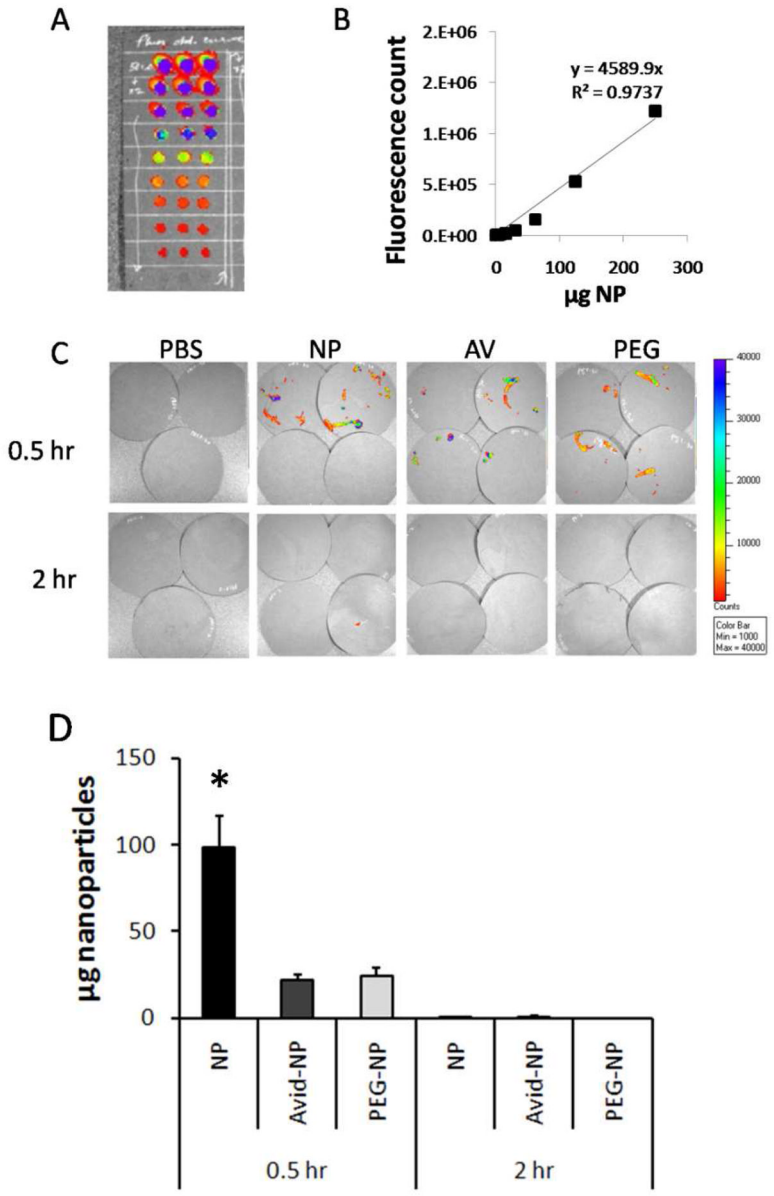

Figure 3.

Measurement of particle leakage from mice after ivag administration. (A) Fluorescence particles deposited on black absorbent paper were visualized using the IVIS 200 system. (B) A standard curve made from known amounts of particles was used to convert measured fluorescence signals to µg nanoparticles. For each animal, the paper lining was changed once after 0.5 hrs, and this second lining was removed at 2 hrs post initial time of delivery. (C) Images were taken in sets of 3–4 papers. Between 20–100 µg nanoparticles were found on absorbent papers within the first 0.5 hrs, no particles were found on the paper collected after 2 hrs. (D) The NP formulation displayed the highest degree of leakage, approximately 5x greater than Avid-NP and PEG-NP formulations; * Denotes significant difference between sample and remaining groups within similar time point, $p < 0.0005$.

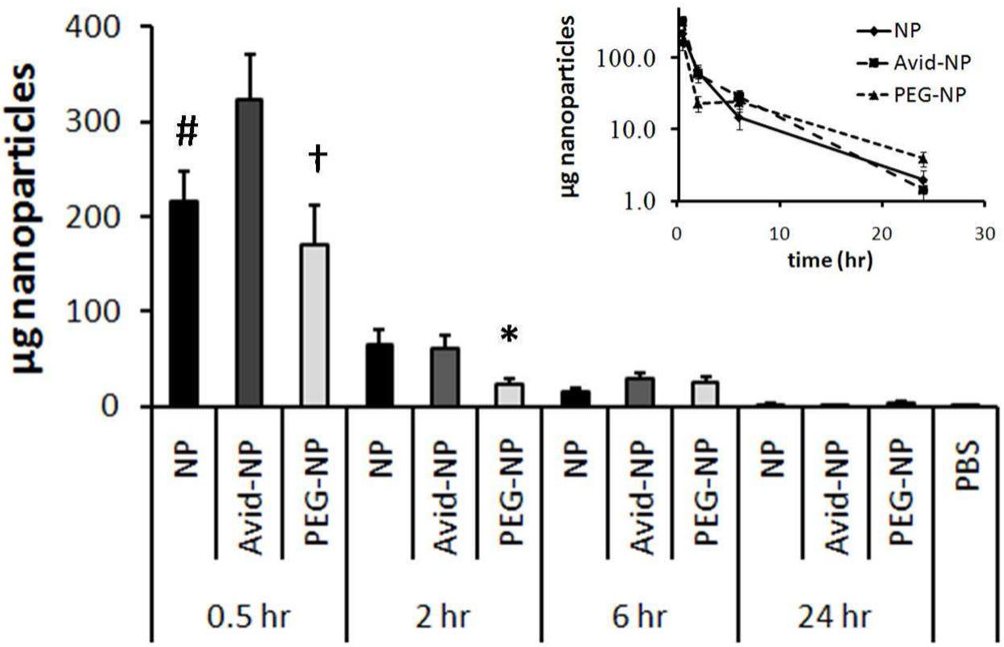

Figure 4.

Measurement of particles collected by vaginal washing. Fluorescent particles were recovered from lumen of the reproductive tract by lavages at 0.5, 2, 6 or 24 hrs after delivery. Quantities of particles recovered within the washes decreased over the period of sampling. On average, Avid-NP and NP displayed higher lumen retention than PEG-NP. Particle concentrations from vaginal washes were also plotted as a function of time on a semi-log scale to demonstrate the kinetics of nanoparticle association with mucus gel (inset). Significant differences between formulations were found at both 0.5 and 2 hrs.

# denotes difference with Avid-NP at 0.5hr, $p < 0.10$

+ denotes difference with Avid-NP at 0.5 hr, $p < 0.025$

* Denotes significant difference between sample and remaining groups within similar time point, $p < 0.025$

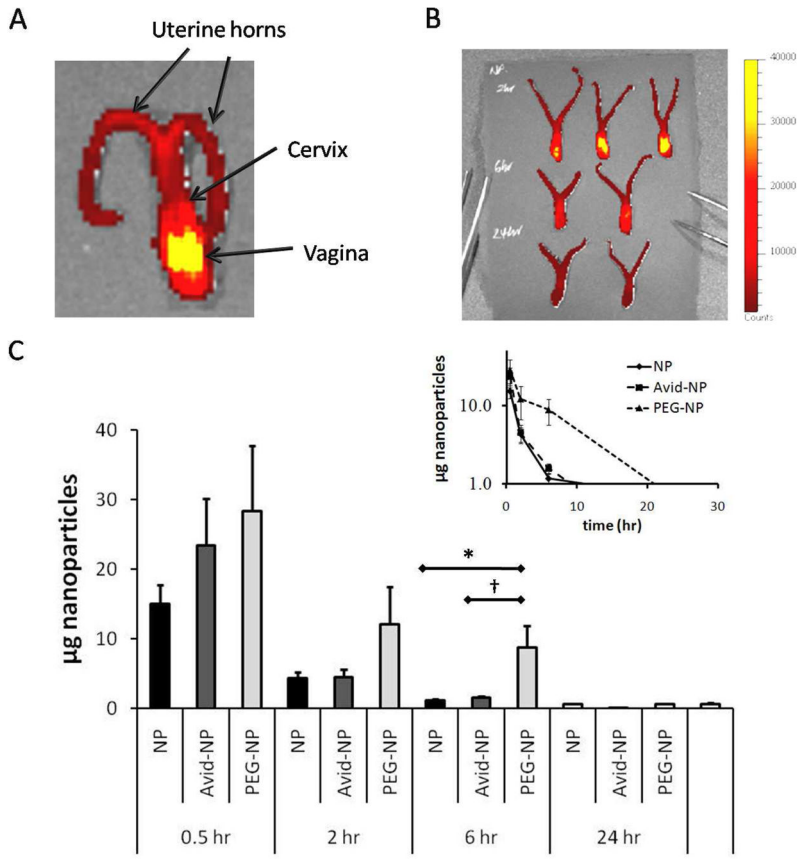

Figure 5.

Measurement of particles within tissue. (A) After ivag administration, the majority of particles were found in the lower reproductive tract (vagina), but not the cervical region or uterine horns. (B) Over the first 24 hrs, most particles remain in the vaginal tract; however, the total concentration decreases substantially. (C) Extracted fluorescence from harvested mice reproductive tissues revealed a similar trend as the whole organ images, in which particle concentration within the tissue decreased over time. Particle concentration in tissue was also plotted as a function of time on a semi-log scale to demonstrate the kinetics of nanoparticle disappearance from the vaginal washes (inset). On average, PEG particle formulations displayed higher tissue retention across all measured time points, as compared to NP and Avid-NP. This enhanced tissue retention is statistically significant at 6 hrs.

* denotes $p < 0.042$

† denotes $p < 0.053$

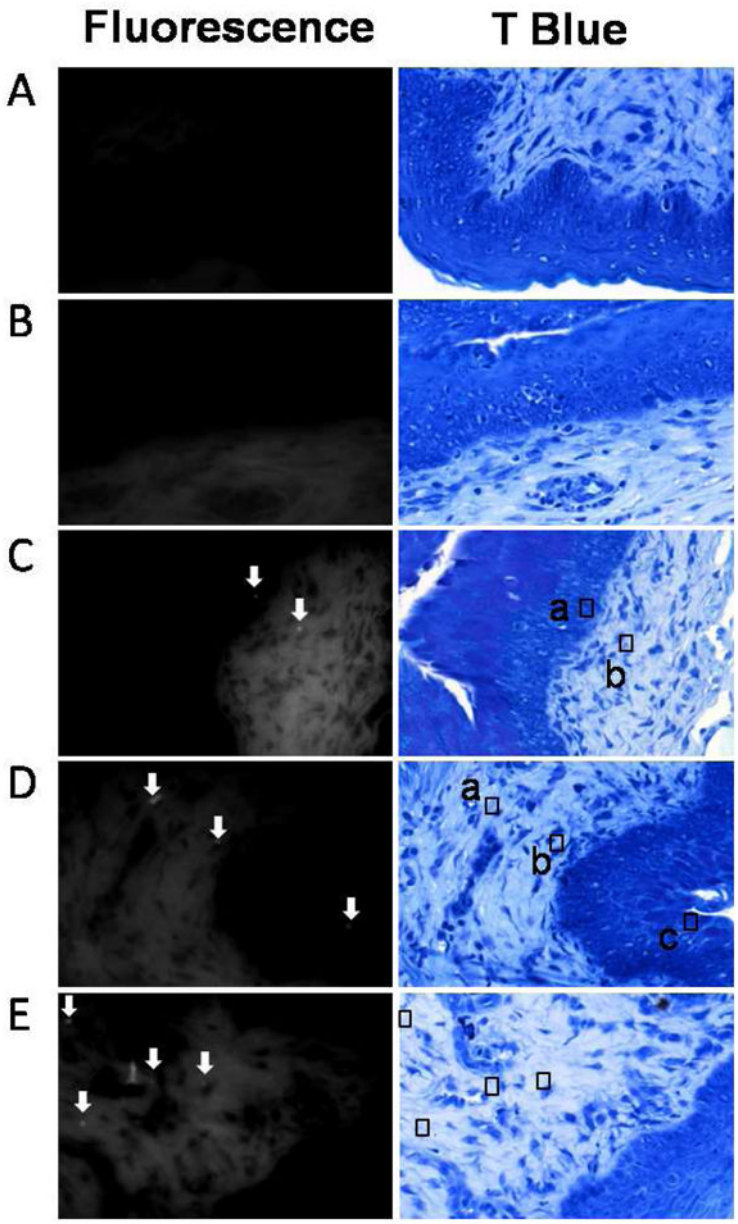

Figure 6.

Fluorescent and T Blue images of representative vaginal tissue sections from mice that were (A) untreated, (B) treated with non-fluorescent nanoparticles, (C) NP, (D) Avid-NP and (E) PEG-NP. For each section, two images were provided: a fluorescent image that shows the presence of C6-loaded particles, and a brightfield image of the same section stained with T Blue, to enable classification of cell populations within the tissue. Fluorescent particles appeared as bright dots (indicated by solid white arrows) on the left image, and their respective positions and association with different cell types (boxed) was seen on the right image. No fluorescence was found in tissues from control animals (A, B). For tissues from animals treated with C6-loaded particles (C,D,E) the labeled boxes indicate the types of cells in the region of particle fluorescence: Sample C: **a** = epithelial cell, **b** = submucosal stromal cell; sample D: **a** = fibroblast cell, **b** = submucosal stromal cell, **c** = epithelial cell; sample E: all are submucosal stromal cells.

Table 1

Particle quantity (μg) recovered from blot, lavage and tissue extracts at specific time points.

		Blot (μg C6NP)			Lavage (μg C6NP)			Extract (μg C6NP)		
	samples	**n**	**Average ± SEM**	**median**	**n**	**Average ± SEM**	**median**	**n**	**Average ± SEM**	**median**
	PBS	25	0	0	9	0.5 ± 0.1	0.4	4	0.6 ± 0.2	0.6
0.5 hr	**NP**	54	99 ± 18	51	8	220 ± 32	240	4	15 ± 2.8	13
	Avid-NP	51	22 ± 3.5	11	9	320 ± 46	330	4	23 ± 6.8	20
	PEG-NP	52	25 ± 4.7	9.7	10	170 ± 41	160	5	28 ± 9.4	25
2 hr	**NP**	28	0.2 ± 0.2	0.0	35	66 ± 15	29	7	4.3 ± 0.9	3.8
	Avid-NP	32	0.5 ± 0.5	0.0	36	60 ± 15	26	8	4.5 ± 1.2	3.1
	PEG-NP	25	0.0	0.0	36	23 ± 5.7	7.4	8	12 ± 5.4	4.0
6 hr	**NP**	-	-	-	16	15 ± 4.7	4.4	7	2.0 ± 0.2	1.0
	Avid-NP	-	-	-	19	29 ± 6.4	31	7	1.6 ± 0.2	1.7
	PEG-NP	-	-	-	19	24± 6.6	3.5	8	8.8 ± 3.1	4.2
24 hr	**NP**	-	-	-	9	2.0 ± 0.7	0.9	5	0.7 ± 0.1	0.7
	Avid-NP	-	-	-	9	1.4 ± 0.4	0.8	5	0.1 ± 0.0	0.1
	PEG-NP	-	-	-	8	3.9 ± 0.9	2.7	5	0.6 ± 0.0	0.7

J Control Release. Author manuscript; available in PMC 2012 December 10.

Table 2

Total particles recovered at 0.5 and 2 hrs

		total recovered	%
0.5 hr	NP	330	44%
	Avid-NP	370	49%
	PEG-NP	220	30%
2 hr	NP	170	22%
	Avid-NP	87	12%
	PEG-NP	60	8%